DOI: 10.1002/ejic.200700946

Synthesis of Soluble and Size-Controlled SnO_2 and CeO_2 Nanocrystals: Application of a General Concept for the Low-Temperature, Hydrolytic Synthesis of Organically Capped Oxide Nanoparticles

Mauro Epifani,*[a] Jordi Arbiol,[b,c] Teresa Andreu,[b] and Joan R. Morante[b]

Keywords: Sol–gel processes / Synthesis design / Colloids / Nanostructures

Metal oxide (CeO_2, SnO_2) sols were prepared in such a way as to hinder the inorganic condensation reactions. Acetylacetone was added to cerium nitrate solutions before hydrolysis with ammonia solution, while solvolysis of anhydrous tin chloride with methanol was used for preparing SnO_2 sols. The sols were then injected into dodecylamine at 160 °C, followed by heating at the resulting temperature for 1 h. A clear sol was obtained, from which the products were extracted by precipitation with methanol and dried. Analysis by X-ray diffraction and TEM demonstrated the presence of CeO_2 and SnO_2 nanocrystals, whose size depended on the metal concentration in the starting sol, ranging from 2.6 to 3.5 nm for CeO_2 and from 1 to 1.9 nm for SnO_2. The nanocrystals were soluble after the synthesis and redispersable in organic solvents, forming stable suspensions. The process appears to be easily generalizable to systems having similar hydrolytic chemistry.

Introduction

The synthesis of oxide nanocrystals is currently under intensive development, and general trends begin to appear in the various synthetic approaches that have been introduced. A general direct route to soluble oxide nanocrystals relies on the high-temperature decomposition of fatty acids, metal salts, and other, even inorganic, precursors,[1] while high-quality nanocrystals can also be obtained from the solvolytic processing of metal alkoxides and acetylacetonates[2] and can be redispersed in a solvent after a suitable surface functionalization.[3] While the currently available syntheses offer remarkable results in terms of size dispersion, generality and processability, the investigation of alternative formation mechanisms of such nanostructures is of remarkable fundamental interest. In a recent work,[4] we have developed a hydrolytic synthesis of metal oxide nanocrystals based on the injection at 160 °C of metal oxide sols into coordinating solutions composed of tetradecene and an alkylamine. In general, the synthesis product is not directly redispersable in a solvent, also as a consequence of the low amine concentration. In this work we present a different synthetic approach, where the amine constitutes the only component of the injection solution. Far from completely hindering nanoparticle formation, the amine instead allows the easy preparation of completely soluble and stable oxide nanocrystals, and the control of the metal concentration in the starting sol allows readily tuning the final nanocrystal size. The process was tested on SnO_2 and CeO_2 nanocrystals, and while the crystalline nature of the final product has to be established in each case because of the very fast particle formation kinetics, the general synthetic scheme can be applied in all the cases where a similar hydrolytic chemistry can be exploited.

Results and Discussion

In our previous work, the amine had the double function of catalyzing the condensation of the oxide species present in the starting sol and of avoiding their uncontrolled growth by bonding to the surface metal ions on the growing nanoparticles. The amine was originally meant as a component of the injection solution with such precisely determined functions, but from a thorough investigation of the pathways of nanoparticle formation, it appeared that the whole process is extremely complex, and, among the factors influencing it, mass transport of the amine in the solution is essential: if a solvent capable of strongly bonding with the amine is used in the injection solution, almost no particle formation occurs. This effect suggested the exploitation of the amine from the point of view of the transport of the

[a] Consiglio Nazionale delle Ricerche, Istituto per la Microelettronica ed i Microsistemi (C.N.R.–I.M.M.),
Via Monteroni, 73100 Lecce, Italy
Fax: +39-0831-519106
E-mail: mauro.epifani@le.imm.cnr.it
[b] EME/CeRMAE/IN^{2}UB, Departament d'Electrònica, Universitat de Barcelona,
C. Martì i Franqués, 1 08028 Barcelona, CAT, Spain
[c] TEM-MAT, Serveis Cientificotècnics, Universitat de Barcelona,
C. Lluìs Solè I Sabaris 1, 08028 Barcelona, CAT, Spain

Supporting information for this article is available on the WWW under http://www.eurjic.org or from the author.

metal oxide species: if the amine concentration is increased until it becomes the only component of the injection solution, will it completely hinder particle formation by forming complexes with all the metal oxide species? It is not straightforward to get a foresight for such an experiment: in addition to the just mentioned effect of the amine as a solvent, it is also possible that isolated regions of metal oxide sols are formed upon sudden injection, which are rapidly condensed by the amine medium to form nanoparticles. Thus, a direct assessment was carried out by injecting sols of CeO_2 and SnO_2, as case studies of nitrate- and chloride-derived sols, respectively, as described in the Experimental Section. A further advantage is that such systems provide nanocrystalline products in very mild temperature conditions. Before exposing the results, a further consideration is necessary for clarifying the theoretical background of the process. Let us suppose that separated metal oxide regions are formed upon sol injection and that their volume is not influenced by the processing parameters of the starting sol, in particular by the metal concentration. Then, if the metal concentration in the starting sol is changed, such regions will have a different metal oxide content in the same volume, and, upon condensation, differently sized nanocrystals will be obtained, since a different content of oxide species is present in each region. Finally, the amine layer external to the metal oxide region will provide solubility. The investigation whether the actual synthetic process really achieves the just proposed imaginative scheme is the aim of the current efforts, but the first results are extremely promising in the direction of preparing soluble, size-controlled nanocrystals in very mild conditions.

In Figure 1 the X-ray diffraction (XRD) patterns are reported for CeO_2 nanoparticles prepared by changing the methanol volume in the starting sol. The reflections of the cubic phase of CeO_2 are clearly seen, and from visual inspection of the peaks, it is clear that by increasing the methanol volume (V_S value) in the starting sol preparation smaller particles are obtained, resulting in peak broadening. From the analysis of the XRD peaks by applying the Scherrer equation to the lowest-angle peak, it is indeed seen that the size increases from 5 to 5.5 to 8.1 nm when V_S is decreased from 10 to 6 to 3 mL, respectively. These results demonstrate the successful design of the synthesis toward the size control of the nanocrystals. The nanocrystals extracted from the reaction pot are fairly soluble in toluene (see Experimental Section), because of a capping layer containing both dodecylamine and acetylacetone (see Figure S1 in the Supporting Information). For obtaining more detailed information about the structure and the morphology of the nanocrystals, the sample prepared with V_S = 3 mL was analyzed by TEM, and the results are shown in Figure 2. Nanoparticles with a mean size of 3.5 ± 0.8 nm (the related size histogram is reported in the Supporting Information) are observed, which are crystallized in the CeO_2 cubic structure. Because of the drying of the sample during the preparation for the TEM observations, the particles are accumulated in some regions, but each nanocrystalline structure is well distinguished from the surroundings, confirming the effect of the capping layer. In some cases, as that shown in the high-resolution image, nanoparticles have coalesced or merged, forming a bigger entity, in this case composed of four previously 2–3 nm nanoparticles. The merged nanoparticles adopt the same crystalline orientation, assuring perfect crystal fusion.

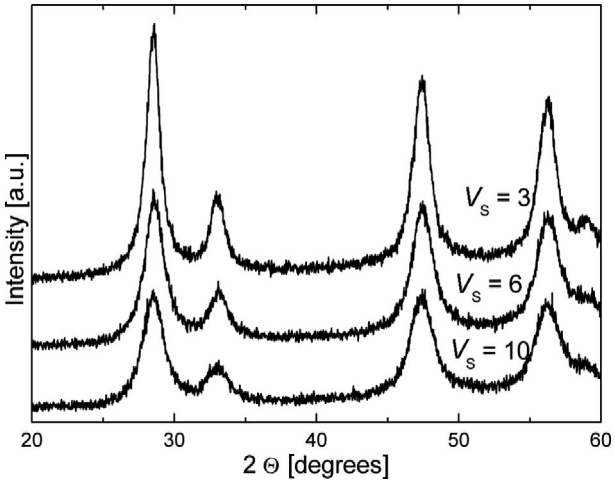

Figure 1. XRD patterns measured on CeO_2 nanocrystals prepared with the indicated V_S values (see Experimental Section).

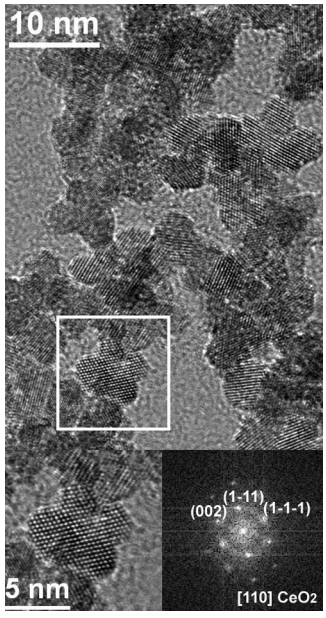

Figure 2. General TEM view of the CeO_2 nanocrystals prepared with V_S = 3 mL. The inset at the bottom shows a high-resolution image of the marked region and the related power spectrum.

The discrepancy between the XRD and TEM size is attributed to the fact that the XRD probe cannot distinguish between such merged crystalline domains. For ensuring actual size control the nanocrystals prepared with V_S = 10 mL, were also investigated by TEM and found to have a mean size of 2.6 ± 0.7 nm (Figure S4, Supporting Information). In Figure 3, the XRD patterns measured on similarly prepared SnO_2 nanocrystals are reported, from which the presence of nanocrystalline structures is again inferred.

A size increasing from 1 to 1.5 nm is deduced when V_S is changed from 10 to 3 mL. A direct observation of the nanocrystals was also necessary in this case, and in Figure 4 the results are reported for the sample prepared with V_S = 3 mL.

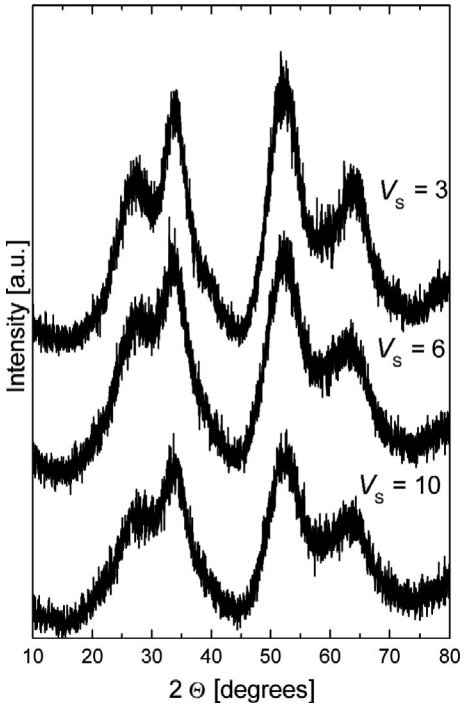

Figure 3. XRD patterns measured on SnO_2 nanocrystals prepared with the indicated V_S values (see Experimental Section).

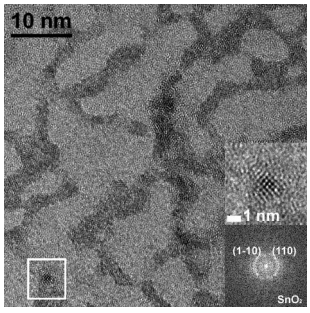

Figure 4. General TEM view of the SnO_2 nanocrystals prepared with V_S = 3 mL. The inset at the bottom shows a high-resolution image of the marked region and the related power spectrum.

Threading nanostructures and nanoparticles embedded on the chains can be observed in this sample. The mean size is 1.9 ± 0.3 nm (the related size histogram is reported in the Supporting Information). As observed from HRTEM micrographs, nanoparticles crystallize in the SnO_2 rutile structure. However, there is a high crystalline distortion. Figure 4 shows a nanoparticle which presents (110) and (1–10) SnO_2 planes with 0.335 nm interplanar distance. However, the angle between the two planes is 78°, far from the 90° that would correspond to a perfect rutile structure visualized along the [001] zone axis. This effect may indeed be related to the very small size of the nanoparticles. In the case of SnO_2, again soluble nanocrystals are obtained. The size control is less evident, and from our previous study,[4] it is due to the limited hydrolysis of the precursor, in turn due to the residual chlorine bonded to tin. This result shows that the synthesis scheme is indeed very general and easily modified for other systems, but the crystalline state of the final product may require some further treatment for obtaining full crystallization.

Conclusions

Soluble, size-controlled CeO_2 and SnO_2 nanocrystals were prepared by injecting the corresponding sol in dodecylamine at 160 °C. The size control was carried out in a simple manner by just modifying the metal concentration in the starting sol. The resulting nanocrystals were soluble in organic solvents, forming stable suspensions. The process was studied for systems representing the use of metal nitrates and anhydrous chlorides in the preparation of metal oxide sols. It represents a general processing approach for systems having a similar hydrolytic chemistry. The crystalline state of the final product depends on the specific system and may require further treatment to obtain fully crystallized nanostructures.

Experimental Section

CeO_2 sol was prepared by dissolving $Ce(NO_3)_3{\cdot}6H_2O$ (2.6 mmol) in a methanol volume indicated with V_S, ranging from 3 to 10 mL. To the resulting clear solution, acetylacetone was added with an acacH/Ce molar ratio of 3. After 1 h, an ammonia solution in water (30 wt.-%) was dropped in the sol, followed by vigorous stirring for a further 24 h. The NH_3/Ce molar ratio was 0.6. For preparing the SnO_2 sol, anhydrous $SnCl_4$ (3.9 mmol) was treated with a methanol volume indicated by V_S, ranging from 3 to 10 mL, in a glovebox, with evolution of heat and vapors. After 1 h, water was added with a H_2O/metal molar ratio of 16. In a 500-mL flask thoroughly degassed with nitrogen, dodecylamine (10 mL) was heated up to 160 °C, then CeO_2 or SnO_2 metal oxide sols (2 mL) prepared with various V_S values were injected into the flask through a septum. The solution temperature dropped to 80–100 °C, depending on the system, and was kept at that value by decreasing the power supply to the flask heater. After 2 h, the flask was cooled. Clear suspensions were obtained, and methanol addition resulted in precipitation. The nanocrystals were recovered by centrifugation, and at this stage were fairly soluble in toluene, yielding stable suspensions with a solid concentration of at least 35–45 mg/mL, depending on the system and the conditions of synthesis. The nanocrystals, further washed with methanol, were not perfectly soluble in toluene any more and could be redispersed after adding 150–300 μL of dodecylamine or trioctylphosphane. After being dried at 90 °C, the extracted nanocrystals were characterized by X-ray diffraction (XRD) with a Panalytical Alfa diffractometer with the Cu-K_α1 radiation (λ = 1.5406 Å). The structural and morphological characterization of the nanocrystals was carried out by means of transmission electron microscopy (TEM). In order to obtain the high-resolution TEM (HRTEM) results, we used a field emission gun microscope, Jeol 2010F, operated at 200 kV and with a point-to-point resolution of 0.19 nm. The softwares used for digital image analysis and crystallographic indexation were the Digital Micro-

graph (Gatan) and Carine, respectively. The samples for the TEM observations were prepared by placing a drop of nanocrystal suspension in toluene onto a carbon-coated copper grid, followed by drying.

Supporting Information (see footnote on the first page of this article): FTIR curve on CeO_2 nanocrystals, size histograms, and further TEM images.

Acknowledgments

The XRD unit of the Serveis Cientificotecnics of the University of Barcelona is gratefully acknowledged for its cooperation. This work was supported by the European Union in the frame of the NANOS4 (Grant NMP4-CT-2003–001528) project.

[1] a) J. Rockenberger, E. C. Scher, A. P. Alivisatos, *J. Am. Chem. Soc.* **1999**, *121*, 11595–11596; b) S. Sun, H. Zeng, *J. Am. Chem. Soc.* **2002**, *124*, 8204–8205; c) C. Feldmann, *Adv. Funct. Mater.* **2003**, *13*, 101–107; d) J. Park, K. An, Y. Hwang, J.-G. Park, H.-J. Noh, J.-Y. Kim, J.-H. Park, N.-M. Hwang, T. Hyeon, *Nat. Mater.* **2004**, *3*, 891–895; e) N. R. Jana, Y. Chen, X. Peng, *Chem. Mater.* **2004**, *16*, 3931–3935; f) J.-w. Seo, Y.-w. Yun, S. J. Ko, J. Cheon, *J. Phys. Chem., B* **2005**, *109*, 5389–5391; g) J. Park, E. Lee, N.-M. Hwang, M. Kang, S. C. Kim, Y. Hwang, J.-G. Park, H.-J. Noh, J.-Y. Kim, J.-H. Park, T. Hyeon, *Angew. Chem. Int. Ed.* **2005**, *44*, 2872–2877; h) Y. Lee, J. Lee, C. J. Bae, J. G. Park, H.-J. Noh, J.-H. Park, T. Hyeon, *Adv. Funct. Mater.* **2005**, *15*, 503–509; i) T. Yu, J. Joo, Y. I. Park, T. Hyeon, *Angew. Chem. Int. Ed.* **2005**, *44*, 7411–7414; j) Y.-W. Jun, J.-S. Choi, J. Cheon, *Angew. Chem. Int. Ed.* **2006**, *45*, 3414–3439; k) K. An, N. Lee, J. Park, S. C. Kim, Y. Hwang, J.-G. Park, J.-Y. Kim, J.-H. Park, M. J. Han, J. Yu, T. Hyeon, *J. Am. Chem. Soc.* **2006**, *128*, 9753–9760; l) H. Gu, M. D. Soucek, *Chem. Mater.* **2007**, *19*, 1103–1110; m) Z. Wang, Z. Quan, J. Lin, *Inorg. Chem.* **2007**, *46*, 5237–5242; n) Q. Liu, W. Lu, A. Ma, J. Tang, J. Lin, J. Fang, *J. Am. Chem. Soc.* **2005**, *127*, 5276–5277; o) Z. Zhuang, Q. Peng, J. Liu, X. Wang, Y. Li, *Inorg. Chem.* **2007**, *46*, 5179–5187.

[2] a) M. Niederberger, G. Garnweitner, N. Pinna, M. Antonietti, *J. Am. Chem. Soc.* **2004**, *126*, 9120–9126; b) M. Niederberger, N. Pinna, J. Polleux, M. Antonietti, *Angew. Chem. Int. Ed.* **2004**, *43*, 2270–2273; c) N. Pinna, G. Garnweitner, M. Antonietti, M. Niederberger, *J. Am. Chem. Soc.* **2005**, *127*, 5608–5612; d) G. Garnweitner, J. Hentschel, M. Antonietti, M. Niederberger, *Chem. Mater.* **2005**, *17*, 4594–4599; e) N. Zhao, D. Pan, W. Nie, X. Ji, *J. Am. Chem. Soc.* **2006**, *128*, 10118–10124; f) J. Zhang, S. Ohara, M. Umetsu, T. Naka, Y. Hatakeyama, T. Adschiri, *Adv. Mater.* **2007**, *19*, 203–206; g) F. Zhou, X. Zhao, H. Xu, C. Yuan, *J. Phys. Chem., C* **2007**, *111*, 1651–1657; h) S. Zhou, M. Antonietti, M. Niederberger, *Small* **2007**, *3*, 763–767; i) S.-B. Wang, Y.-L. Min, S.-H. Yu, *J. Phys. Chem., C* **2007**, *111*, 3551–3554.

[3] M. Niederberger, G. Garnweitner, F. Krumeich, R. Nesper, H. Cölfen, M. Antonietti, *Chem. Mater.* **2004**, *16*, 1202–1208.

[4] M. Epifani, R. Díaz, J. Arbiol, E. Comini, N. Sergent, T. Pagnier, P. Siciliano, G. Faglia, J. R. Morante, *Adv. Funct. Mater.* **2006**, *16*, 1488–1498.

Received: September 10, 2007
Published Online: December 6, 2007

